Copyright Notice

(Article begins on next page)

Comparing resonant photon tunneling via cavity modes and Tamm plasmon polariton modes in metal-coated Bragg mirrors

K. Leosson,[1,*] S. Shayestehaminzadeh,[1] T. K. Tryggvason,[1] A. Kossoy,[1] B. Agnarsson,[1,2] F. Magnus,[1,3] S. Olafsson,[1] J. T. Gudmundsson,[1,4] E. B. Magnusson,[1] and I. A. Shelykh[1,5]

[1]*Science Institute, University of Iceland, Dunhagi 3, IS-107 Reykjavik, Iceland*

[2]*Department of Applied Physics, Chalmers University of Technology, SE-41296 Gothenburg, Sweden*

[3]*Department of Physics and Astronomy, Materials Physics Division, Uppsala University, SE-75120 Uppsala, Sweden*

[4]*University of Michigan—Shanghai Jiao Tong University Joint Institute, 200240 Shanghai, China*

[5]*Division of Physics and Applied Physics, Nanyang Technological University, 637371 Singapore*

**Corresponding author: kleos@hi.is*

Received June 28, 2012; revised August 20, 2012; accepted August 22, 2012;
posted August 24, 2012 (Doc. ID 171475); published September 21, 2012

Resonant photon tunneling was investigated experimentally in multilayer structures containing a high-contrast (TiO_2/SiO_2) Bragg mirror capped with a semitransparent gold film. Transmission via a fundamental cavity resonance was compared with transmission via the Tamm plasmon polariton resonance that appears at the interface between a metal film and a one-dimensional photonic bandgap structure. The Tamm-plasmon-mediated transmission exhibits a smaller dependence on the angle and polarization of the incident light for similar values of peak transmission, resonance wavelength, and finesse. Implications for transparent electrical contacts based on resonant tunneling structures are discussed.

OCIS codes: 230.4170, 240.6690, 230.1480, 310.6188, 310.7005.

An interesting and useful feature of optical and electronic systems is the resonant tunneling phenomenon [1,2], where transmission through a double finite potential barrier or a pair of mirrors with <100% reflectivity can become larger than transmission through a single barrier, provided that the energy of the incident radiation is resonant with a quasi-bound state between the two barriers. In optics, the double barrier can be provided by a pair of semitransparent metal mirrors, as in the case of the classic Fabry–Pérot etalon or by a pair of distributed Bragg reflectors (DBRs), as is typical of one-dimensional microcavity structures [3]. At resonance, there is a buildup of energy in the cavity and back-reflected light destructively interferes, giving up to 100% transmission through the structure, in the absence of optical loss. Recently, a new type of optical interface resonance in a metal-coated DBR (in the absence of a cavity) was predicted [4] and experimentally verified [5]. The resonance occurs within the stop band of the Bragg mirror and has been referred to as a Tamm plasmon polariton (TPP), by analogy with the electronic Tamm surface states. TPPs are currently being investigated for a variety of applications [5–7].

Resonant photon tunneling (RPT) through metal-dielectric structures provides a route to realizing electrical contacts with high conductivity, providing substantially larger optical transmission than through the metal film alone (within a wavelength range defined by the energy and lifetime of the quasi-bound state). Highly conductive metals such as gold or silver are promising as transparent contact materials, but in the thin-film limit, both optical transmission and conductivity are limited by the self-organization of nanoscale islands [8]. It is therefore of interest to be able to increase transmission for certain wavelengths while maintaining a relatively large film thickness for providing low contact resistance. Furthermore, it is important to minimize the angular dependence (hue) of optical transmission through such transparent electrodes. Here, we compare RPT through two types of low-finesse metal-dielectric resonators, one supporting a TPP interface state and the other supporting a conventional $\lambda/2$-cavity mode. In order to realize a dielectric mirror with a spectrally wide stop band, we used TiO_2 and SiO_2 to provide a large index contrast ($n = 2.59$ and 1.45, respectively, at the center of the stop band). The two classes of investigated structures are based on similar dielectric mirrors, as shown schematically in Fig. 1, with a low-index cavity layer or a high-index spacer layer added on top of the dielectric mirror, and capped with gold layers of varying thickness.

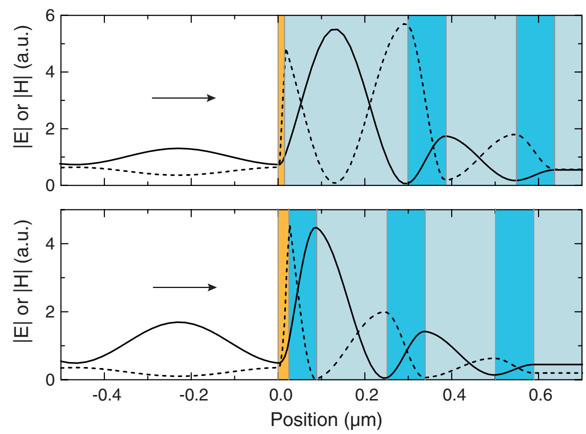

Fig. 1. (Color online) Electric (solid curves) and magnetic (dashed curves) field amplitudes in the cavity geometry (top) and the Tamm plasmon polariton geometry (bottom), for light at the resonance wavelength (950 nm) incident from the left. Light blue and dark blue shading indicates low-index (SiO_2 or PMMA) and high-index (TiO_2) dielectric layers, respectively. Thin orange layers represent gold.

0146-9592/12/194026-03$15.00/0

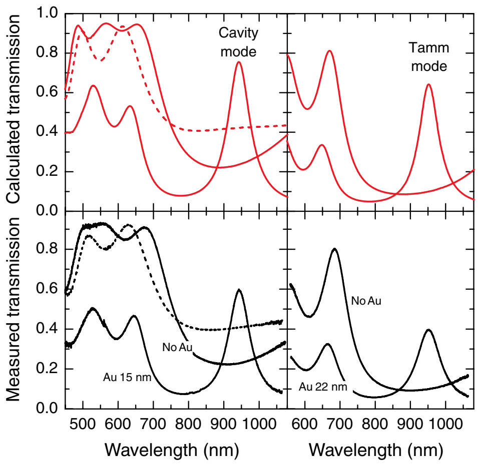

Fig. 2. (Color online) Calculated (top) and measured (bottom) transmission curves for the two-period Bragg mirror alone (dashed curves), cavity structure (left panels), or TPP structure (right panels) before and after application of the metal layer (cf. Fig. 1). Both structures were designed to give resonant transmission at around 950 nm wavelength (at the center of the stop band of the Bragg mirror). All curves include an incoherent backside reflection of about 4%.

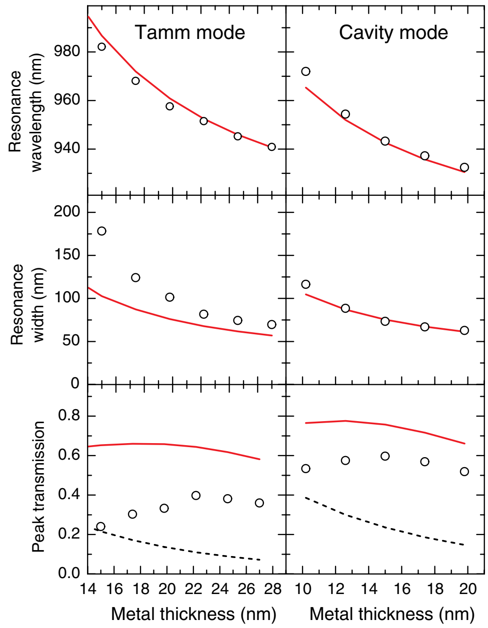

Fig. 3 (Color online) Calculated (solid curves) and experimental (symbols) values for spectral position, spectral width, and optical transmission at resonance at normal incidence. The dashed curves show the value of optical transmission expected through a correspondingly thick smooth gold film deposited directly on glass.

We fabricated Bragg mirrors on fused-silica substrates by reactive high-power impulse magnetron sputtering (HiPIMS) [9] and reactive dc magnetron sputtering (dcMS), for the TiO_2 and SiO_2 layers, respectively. Ti and Si targets were used and the sputtering gas was a mixture of argon (37 sccm) and oxygen (1.2 sccm) at a total pressure of 0.7 Pa. Before deposition, the substrate was baked at 600 °C for 10 min. During deposition, the substrate temperature was maintained at 500 °C. For HiPIMS, power was supplied by a SPIK 1000A pulse unit (Melec GmbH), operating in the unipolar negative mode at a constant voltage (pulse length 200 μs, pulse frequency 75 Hz, and pulse amplitude 860 V). The HiPIMS discharge was maintained in metal mode for 76 min to achieve 88 nm thickness of TiO_2. SiO_2 film deposition was carried out by dcMS in constant-power mode at 100 W using an Advanced Energy MDX500 power supply. The dcMS discharge was kept in metal mode for 74 min with 282–285 mA average discharge current to obtain 163 nm thick SiO_2. Further details of the fabrication and material properties will be reported elsewhere. The above process was repeated twice, to obtain a two-period DBR with approximately 40% transmission within the stop band (750–1150 nm), as shown in Fig. 2. Two sets of structures were fabricated on identical Bragg mirrors, using (i) a 122 nm thick PMMA layer (approximately index-matched to the SiO_2), spin-coated and baked at 180 °C, and (ii) a 64 nm thick layer of TiO_2 (deposited as above). Gold deposition (thickness range 10–27 nm) was carried out by conventional e-beam evaporation, and an accurate thickness calibration was performed using X-ray reflectivity measurements.

Optical transmission spectra were measured using an unpolarized collimated white-light source (halogen lamp), spectrometer (PI SpectraPro SP-2356, 150 l/mm grating), and CCD camera (Pixis:100F). Corresponding calculations were carried out with a general transfer-matrix method, described, e.g., in [10], using refractive index values measured with spectroscopic ellipsometry on single layers of TiO_2 or SiO_2 grown under identical conditions. For gold, values provided by Johnson and Christy [11] were used. In all calculations, an incoherent 4% reflection at the back side of the fused silica substrate was included. Figure 2 compares calculated and measured values of optical transmission through the two-period DBR alone, through the DBR with cavity layer or high-index spacer layer, and through complete gold-capped structures. For the cases shown, RPT is expected to give increased transmission over a bandwidth of ≈100 nm, as compared to transmission through the gold film alone, up to approximately 3× (cavity mode) or 6× (Tamm mode) transmission enhancement at the resonance peak. In both cases, spacer layer and metal film thickness were chosen to maximize the height of the resonant transmission peak and to position it close to the center of the stop band. Experimental curves show a lower peak transmission than expected, as discussed in more detail below, but are otherwise in good agreement with the theoretical prediction. The resonance peaks are well described with a Lorentzian line shape, both in the theoretical and experimental spectra.

Experimental data on the resonance position, spectral width (FWHM), and peak transmission (all derived from Lorentzian fits to experimental data) for different values of the gold film thickness, at normal incidence, are compared with theoretical values in Fig. 3. The experimentally observed lifetime of the TPP is shorter than expected, especially for lower metal film thickness (≲20 nm). Also, measured peak transmission is substantially lower than expected for all values of the gold film thickness, especially in the case of the TPP structure.

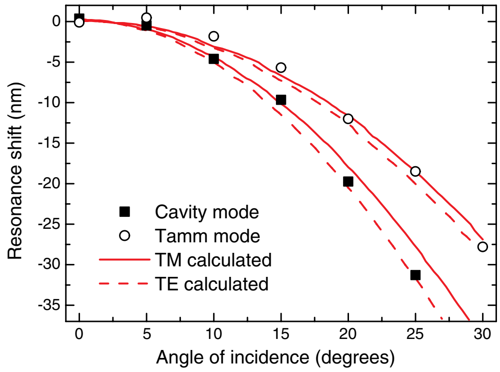

Fig. 4. (Color online) Angular shift in peak resonant transmission wavelength for unpolarized light for the cavity mode structure (solid squares) and the Tamm plasmon polariton structure (open circles). Solid and dashed curves show corresponding transfer-matrix calculations for TM and TE polarized light, respectively.

Nevertheless, significantly enhanced optical transmission at resonance was confirmed, up to 3.5× (cavity mode) or 5.0× (TPP mode) larger than through a correspondingly thick gold film for the thickest gold films. We believe that the observed deviations from theoretical predictions in the case of the TPP structure arise mainly from the roughness of the TiO_2-gold interface. Atomic force microscope measurements on the completed TPP structure revealed a substantial roughness (4.4 nm RMS) with a length scale that correlates well with the size of individual TiO_2 crystals. Further process optimization is required to achieve subnanometer roughness, as has been achieved for individual TiO_2 layers [12].

The position of the RPT maximum depends on the incident angle, due to increasing optical path lengths through the structure. This dispersion behavior may be described by introducing an effective photon mass in the transverse direction, m^*, associated with the cavity mode. The angular dependence of RPT through the two types of investigated structures is shown in Fig. 4. Experimental data were collected with unpolarized light, but theoretical curves are shown separately for TE and TM polarization. In the case of the TPP structure, the angular dependence is clearly reduced, corresponding to a 50% increase in transverse effective photon mass, as compared to the cavity mode (DBR–metal or DBR–DBR). Also, polarization dependence is smaller in the case of the TPP mode, with $(m^*_{\mathrm{TE}} - m^*_{\mathrm{TM}})/(m^*_{\mathrm{TE}} + m^*_{\mathrm{TM}}) = 3.5\%$, compared to 6.6% for the DBR–metal cavity mode.

In summary, we have shown that optical transmission through metal films can be substantially enhanced by RPT in a metal-coated Bragg mirror. Resonant transmission via the Tamm plasmon polariton interface state shows lower angular dependence and lower polarization dependence than transmission via a conventional cavity mode having a similar wavelength and finesse, making the TPP state interesting in the context of transparent electrical contacts. The high-index-contrast Bragg mirrors used in the present study provide substantial TPP mode confinement with only a few periods. Also, they are transparent throughout the visible range and the present findings can be equally applied at shorter wavelengths, provided that metals with a higher plasma frequency, such as silver, are used.

This work was partially supported by the Icelandic Research Fund Excellence Grant No. 100019011.

References

1. M. Born and E. Wolf, *Principles of Optics* (Cambridge University, 1999).
2. L. L. Chang, L. Esaki, and R. Tsu, Appl. Phys. Lett. **24**, 593 (1974).
3. A. Kavokin, J. J. Baumberg, G. Malpuech, and F. P. Laussy, *Microcavities* (Oxford University, 2007).
4. M. Kaliteevski, I. Iorsh, S. Brand, R. A. Abram, J. M. Chamberlain, A. V. Kavokin, and I. A. Shelykh, Phys. Rev. B **76**, 165415 (2007).
5. M. E. Sasin, R. P. Seisyan, M. A. Kaliteevski, S. Brand, R. A. Abram, J. M. Chamberlain, I. V. Iorsh, I. A. Shelykh, A. Y. Egorov, A. P. Vasil'ev, V. S. Mikhrin, and A. V. Kavokin, Superlattices Microstruct. **47**, 44 (2010).
6. H. X. Da, Z. Q. Huang, and Z. Y. Li, Opt. Lett. **34**, 1693 (2009).
7. E. Homeyer, C. Symonds, A. Lemaitre, J. C. Plenet, and J. Bellessa, Superlattices Microstruct. **49**, 224 (2011).
8. J. Meiss, M. K. Riede, and K. Leo, Appl. Phys. Lett. **94**, 013303 (2009).
9. J. T. Gudmundsson, N. Brenning, D. Lundin, and U. Helmersson, J. Vac. Sci. Technol. A **30**, 030801 (2012).
10. C. C. Katsidis and D. I. Siapkas, Appl. Opt. **41**, 3978 (2002).
11. P. B. Johnson and R. W. Christy, Phys. Rev. B **6**, 4370 (1972).
12. F. Magnus, B. Agnarsson, A. S. Ingason, K. Leosson, S. Olafsson, and J. T. Gudmundsson, in *MRS Proceedings* (2011), Vol. **1352**.